Assessment of Semantic Segmentation Models for Landslide Monitoring Using Satellite Imagery in Peruvian Andes

Roy Yali S. **Pablo Fonseca** **Cesar Beltrán**
Pontifical Catholic University of Peru
Lima, PE 15088
{roy.yali, pfonseca, cbeltran}@pucp.edu.pe

Abstract

In the domain of machine learning, one persistent challenge is the availability of ample data, especially pertinent to computer vision. Moreover, this challenge is amplified within the realm of remote sensing, where annotations for addressing problems are frequently scarce. This manuscript critically examines the daunting task of monitoring a geophysical phenomenon —landslides— within the Peruvian landscape, a nation profoundly impacted by such events on a global scale. In this paper, we present three contributions in that direction.

Our first contribution is to expand a well-known satellite imagery dataset targeting landslides. The nucleus of this foundational dataset originates from Asian territories, comprising 3799 meticulously annotated images. However, recognizing the distinct geospatial dynamics of Peru, we embarked on a rigorous exercise to augment this dataset with 838 local scenarios. These additions maintain congruence with the original dataset in terms of attributes and configuration, thereby ensuring both replicability and scalability for future research endeavours.

Our second contribution is an exhaustive assessment of various semantic segmentation models. At the heart of our experimentation lies the U-net architecture, bolstered by the Weighted Cross Entropy + Dice Loss —a loss function acclaimed for its efficacy in segmentation tasks with imbalanced data sets. The empirical findings are illuminating: a rudimentary U-net architecture exhibits a formidable F1-Score of 75.5%, transcending the benchmark score of 71.65% set by the original dataset.

Our third and final contribution is the comprehensive research framework developed for data acquisition, processing pipeline and model training/evaluation. Given this framework has the potential to drive a general applicability of segmentation systems to landslide monitoring systems, and to have a broader reach to the academic community and governmental stakeholders in Latin America and worldwide, we will be making all scripts and experiment details available upon publication, thus, hoping to foster an environment for collaborative scrutiny, discourse, and further advancement.

1 Introduction

Landslide phenomena, undoubtedly perilous geomorphological events, present pronounced challenges in mountain regions worldwide[1]. Particularly, the topography and settlement patterns of Peru render it vulnerable, with numerous establishments precariously situated in high-risk zones. While the multi-faceted intricacies of landslide assessment often impede holistic evaluations, the advent of

37th Conference on Neural Information Processing Systems (NeurIPS 2023).

satellite imagery—specifically through platforms like Sentinel2 and Alos Palsar—offers a promising avenue for discerning and predicting such geological upheavals.

The crux of this research lies in forging a rigorous analytical framework designed to both segment and detect landslides autonomously through the prism of these satellite imageries. By harnessing advanced computational vision techniques and delving deep into machine learning paradigms, we aspire to attain a granular classification of the impacted regions in the montane rainforests of Peru, which is noteworthy, only second to Colombia in the Americas in terms of landslide susceptibility[2].

In recent years, Earth Observation (EO) has emerged as a pivotal discipline impacting various interdisciplinary research areas such as climate change, risk and disaster management, and foresight analysis[3]. Its transformation can be attributed in part to platforms such as Google Earth Engine (GEE)[4] representing a significant milestone in EO, providing researchers with unparalleled access to extensive spatial data repositories and robust computational resources for real-time processing. This groundbreaking innovation in EO has democratized access to expansive data repositories, simultaneously enabling sophisticated machine learning procedures[5]. Our research objective, in this context, is two-fold: geographically, to be able to pinpoint vulnerable zones, pre and post-landslide occurrences; and from a computer vision perspective, there is an emphatic focus on architecting an avant-garde model built on convolutional neural networks. This model is envisaged to streamline the semantic segmentation of satellite imagery, thereby bolstering the efficacy of surveillance systems.

To comprehend the magnitude and gravity of landslides, one must recognize them as unrestrained terrestrial movements of both soil and bedrock, manifesting formidable geological threats[6]. Their monitoring and the subsequent identification of susceptible regions are paramount for effective hazard mitigation. The Unified Global Landslide Database (UGLD) as curated by Gomez (2023)[2] sheds light on this, chronicling 37,946 landslide events and an alarming tally of 185,753 fatalities spanning 161 countries from 1903 to 2020. Within this global purview, Peru's vulnerability stands out, ranking third in landslides per 1000 km^2. Supplemental data sourced from INDECI accentuates this, highlighting that between 2003 and 2021, Peru witnessed 8,347 landslide-related emergencies culminating in 475 tragic fatalities[7].

2 Dataset

Landslides, with their socio-environmental repercussions, have prominently emerged as a critical area of interest within geospatial research. The assimilation and analytical scrutiny of satellite-derived datasets have become an indispensable tool for discerning and monitoring these geophysical occurrences. Given this backdrop, certain dedicated datasets have been architected, specifically aiming to amplify our comprehension and prognostic abilities regarding global landslide occurrences. Two datasets, namely "Landslide4Sense" (L4S) and our Peruvian-adapted counterpart "L4S-PE", warrant particular attention for their comprehensive satellite image capture and labeling.

2.1 The Landslide4Sense (L4S) Dataset

The L4S dataset[8] encompasses landslide imagery harvested from four geographically distinct regions: Iburi-Tobu in Japan, Karnataka in India, Bagmati in Nepal, and Taitung County in Taiwan. This compilation aggregates 3,799 image patches, devoid of georeferencing but integrating 14 spectral bands—comprehensively combining Sentinel-2 spectral bands with elevation data from the ALOS PALSAR satellite[9]. An inherent need to harmonize the spatial resolution of the incorporated satellite products led to a standard pixel size recalibration. Subsequently, every band was resized to ensure a 10-meter per pixel resolution, resulting in image dimensions of 128x128 pixels. These images are meticulously classified under two categories: landslide presence (1) and absence (0).

2.2 The L4S-PE Dataset

Drawing inspiration from the original L4S dataset —primarily oriented towards the Asian context— L4S-PE was conceived to cater to the unique landscape of the Peruvian forest. Retaining the attributes of L4S, including the 12 bands from the Sentinel-2 and the elevation band from the Alos Palsar, the creation of L4S-PE employed a CloudSen12-based pipeline[10]. This approach facilitates the augmentation of a global dataset with local idiosyncrasies, encompassing landslide detection

in specified Peruvian regions, satellite image acquisitions, semi-automated labeling, and sample standardization for segmentation tasks.

2.2.1 Geographic Focus

The analytical focus hones in on three central Peruvian regions: Junin, Pasco, and Huánuco, situated to the east of the Andes where highlands transition into the rainforest. Dominated by wooded terrains, these regions optimize the visual interpretation of optical remote-sensing imagery. Notably, while regions juxtaposed between coastal areas and mountain ranges frequently experience landslides, the aforementioned regions were strategically selected based on their geomorphological characteristics.

2.2.2 Image Fragment Selection

For the raw data composition of L4S-PE, 1,000 Regions of Interest (ROIs) were delineated across the study area, each spanning 150 x 150 meters. These ROIs were ascertained using visual inspection methodologies on the Google Earth platform, cross-referencing with pre-2018 landslide occurrences. Despite the inherent resolution disparities across the bands, a homogenization process was executed to maintain a consistent spatial resolution of 10 meters. Post a rigorous visual quality assessment, the dataset was filtered to 838 image fragments, removing images plagued by cloud cover, sensor noise, or incongruent landscape features.

2.2.3 Labeling Procedure

The image labeling operation leveraged a refined version of the "Intelligence foR Image Segmentation" (Iris)[11] active learning software. This tool streamlines manual image annotation, offering flexibility in analyzing varying band combinations. Each image fragment, measuring 150x150 meters, offers spatial context for the targeted 128x128-meter area. Upon concluding the annotation phase, labeled outputs were exported in the HDF format, primed for integration with machine learning techniques.

2.2.4 Comparative Analysis: L4S vs. L4S-PE

It is crucial to highlight that the geographic characteristics of the L4S patches differ significantly from those of L4S-PE, particularly regarding precipitation, geomorphology, and landslide triggers, as detailed in the L4S study[8]. This variability, coupled with the limited availability of landslide databases for machine learning modeling in Peru, led to the initiation of a local database. This endeavor aims to broaden the understanding of the characteristics of the Andes, a task also undertaken by the HR-GLAD database[12]. However, these latter studies did not include the Andean mountain range in their analyses. In this context, Figure 1 illustrates the data sources for each database (L4S and L4S-PE), indicating the number of patches analyzed and outlining the download process for creating the databases used in this research.

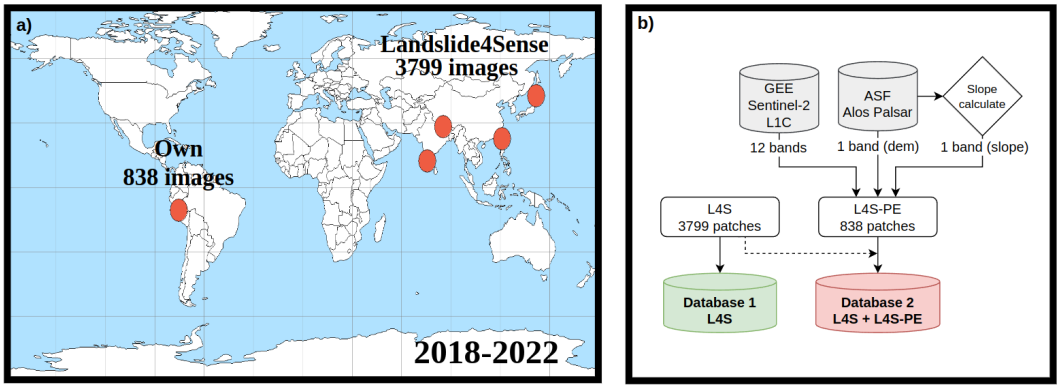

Figure 1: (a) shows the data source, emphasizing the own database (L4S-PE). (b) shows the downloading process and integration to create the two databases evaluated

A comparative exploration was performed between L4S and L4S-PE datasets. Post min-max normalization, pixel distribution across each band was evaluated in the Figure 2. A majority of the

spectral bands exhibited analogous behaviors, with notable variances, especially in Band 1 (Aerosol). Statistical insights revealed a class distribution skewness in both sets: L4S presented a landslide area of 137.56 km² (2.21% landslides, 97.79% non-landslide) while L4S-PE showed 24.71 km^2 (1.8% landslides, 98.2% non-landslide). Despite these disparities, the inherent similarities between the datasets affirm their combined utility in predictive modeling endeavors as we can see in the table 1.

Table 1: Distribution of classes by database, area in square metres of landslides and number of patches for each database. Each patch has 128x128 pixels and 10 metres of spatial resolution.

Source	**Landslide area (km^2)**	**% Landslide / No landslide**	**Number of patches**
L4S	137.56	2.21 / 97.79%	3799
L4S-PE (own)	24.71	1.8 / 98.2%	838
L4S + L4S-PE	162.27	2.14 / 97.86%	4637

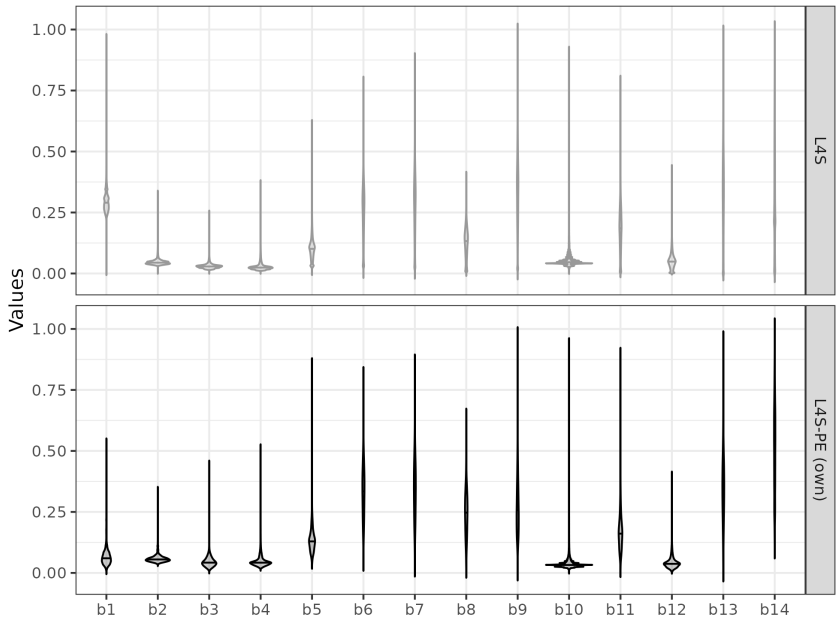

Figure 2: Comparative analysis evaluating distribution and variability for each spectral band values across the datasets L4S and our L4S-PE

By showing similar behaviours in the distributions of both databases, these can be put together in a single database for more extensive modelling purposes. Also, in this study, experiments are performed using different combinations of bands that prioritise the highest resolution (10 metres) corresponding to bands b2, b3, b4, b8, b13 and b14, which, as can be seen in the figure, have no major difference in their distributions.

3 Methodology

In this investigation, our focal point lies in the comparative efficacy of various deep learning models tailored for semantic segmentation. Primarily, these models revolve around the U-net framework[13], augmented by different encoder architectures. The study undertook experiments utilizing two distinct datasets: L4S and an amalgamation of L4S and L4S-PE. Two band combinations were critically evaluated—one encompassing all 14 spectral bands, and another emphasizing the six bands with an original resolution of 10 meters, requiring no down-sampling. These datasets were subsequently stratified into training and validation subsets, and multiple metrics were computed to assess the model performance.

3.1 Loss Functions for Segmentation

- Binary Cross-Entropy (BCE): This quantifies the divergence between the predicted and true probability distributions for individual pixels.
- Weighted Cross-Entropy (WCE): Operating on the same foundational principles as BCE, this introduces a weighting mechanism to address the class imbalance between landslide and non-landslide pixels.

$$\mathcal{L}_{WCE} = -\frac{1}{N}\sum_{i=1}^{n}(\beta Y_i \log \hat{Y}_i + (1 - Y_i)\log(1 - \hat{Y}_i)) \tag{1}$$

- Dice Loss: This metric gauges the overlap between the predicted and reference segmentation masks.

$$\mathcal{L}_{Dice} = 1 - \frac{2 \times |X \cap Y|}{|X| + |Y|} \tag{2}$$

- WCE-Dice Loss: By synergizing the weighted cross-entropy and Dice loss, this function aims to optimize model performance.

$$\mathcal{L}_{WCE-Dice} = (1 - \alpha)\mathcal{L}_{WCE} + \alpha\mathcal{L}_{Dice} \tag{3}$$

3.2 Evaluation Metrics

- Precision: Denotes the proportion of accurately detected landslide areas.
- Recall (Sensitivity): It ascertains the fraction of total landslides in an image that were accurately identified.
- F1-score: Offers a harmonic mean of precision and recall, thereby providing a consolidated metric.
- IoU (Jaccard Index): Quantifies the similarity and diversity between two datasets.

3.3 Experimental Configuration

The computational environment was built with Python 3.8.10 running on Ubuntu 22.04LTS, using an NVIDIA RTX 3070 GPU (16 GB RAM). The deep learning apparatus employed included PyTorch and Pytorch Lightning[14], leveraging the CUDA 12.1 parallel computation platform. Regarding the data implementation, the imagery is sourced from the Google Earth Engine, specifically from Sentinel-2 and Alos Palsar satellites. We analyzed 128x128 pixel images spanning 14 spectral bands from the period 2018-2022, aggregating to a comprehensive 4637 patches. The task of landslide identification was construed as semantic segmentation. Experiments were carried out with the L4S dataset and its combined form with L4S-PE, employing varying spectral band sets. The dataset was separated into experimental subsets—80% allocated for training and 20% for validation, ensuring reproducibility through a consistent random seed.

3.4 Experiments

Within the ambit of landslide segmentation model evaluation, datasets L4S and L4S-PE were deployed, showcasing sample images that delineate the proportions of landslide and non-landslide areas. As mentioned above, experimentation was orchestrated using the PyTorch Lightning and Google Earth Engine (GEE) frameworks. Depending on the specific experiment, either all 14 spectral bands were selected or only those with an intrinsic resolution of 10 meters. Each image was subjected to min-max normalization, scaling values within the 0 to 1 range.

The datasets were bifurcated into training and validation subsets, adhering to an 80/20% ratio. The U-net architecture was the base of all experimental paradigms, with Resnet34 and MobilenetV2 as foundational backbones. The Adam optimizer was embraced with a learning rate of 10^{-3}, and the loss used was WCE-Dice. Learning rates were recalibrated every 30 epochs, and given the data imbalance, a heightened weight was accorded to the landslide class. Should no enhancements materialize after 10 epochs, the model manifesting the lowest validation loss was selected. These experiments are available to see in the Wandb6.

3.5 Results

In our investigation of semantic segmentation in Sentinel2 and Alos Palsar satellite imagery, we evaluated several deep learning models for landslide detection effectiveness. Initially, our evaluation focused on experiments using the L4S dataset, as shown in the table. Our results indicate that working with 14 spectral bands yields slightly better performance compared to using only 6 bands. Furthermore, with an F1 score of 0.755, the Unet (Vanilla) architecture is superior to more complex ones, demonstrating an advantageous trade-off between accuracy and recall. Furthermore, the low Dice-WCE value suggests effective class imbalance management. We also note that an IoU close to 0.60 means a substantial overlap between model predictions and their corresponding labels.

On the other hand, the use of the combined L4S and L4S-PE databases, as can be seen in the table, shows a rather similar, although slightly lower, performance, reaching an F1 score of 0.719. Furthermore, despite the high F1 and Accuracy scores, the performance of the L4S and L4S-PE databases is slightly lower.

Furthermore, despite the high F1 and Accuracy metrics, there is a considerable lag in IoU scores, which is an opportunity to refine the capture of class overlap and to further augment the databases. The following tables list the main metrics and cumulative losses across all the experiments analysed, while figure 3 presents an overview of the visual results.

Table 2: Performance metrics of evaluated models on the validation set of the L4S database

		Metrics				**Loss function**		
		F1-score	**Precision**	**Recall**	**IoU**	**Dice-WCE**	**WCE**	**Dice**
6b	Unet (Vanilla)	**0.747**	0.761	0.739	0.600	**0.223**	0.159	0.287
	Resnet34	0.731	0.784	0.691	0.581	0.238	0.177	0.298
	MobilenetV2	0.718	0.687	0.758	0.565	0.256	0.202	0.309
	Segformer	0.702	0.750	0.672	0.546	0.261	0.196	0.326
14b	Unet (Vanilla)	**0.755**	0.781	0.735	0.611	**0.215**	0.157	0.273
	Resnet34	0.734	0.785	0.695	0.585	0.233	0.174	0.292
	MobilenetV2	0.723	0.735	0.716	0.571	0.246	0.184	0.308
	Segformer	0.714	0.743	0.694	0.559	0.259	0.208	0.310

Table 3: Performance metrics of evaluated models on the combined validation set of the L4S and L4S-PE databases

		Metrics				**Loss function**		
		F1-score	**Precision**	**Recall**	**IoU**	**Dice-WCE**	**WCE**	**Dice**
6b	Unet (Vanilla)	**0.714**	0.749	0.687	0.559	**0.256**	0.191	0.321
	Resnet34	0.695	0.742	0.659	0.537	0.278	0.223	0.333
	MobilenetV2	0.688	0.751	0.640	0.528	0.286	0.237	0.335
	Segformer	0.669	0.712	0.639	0.507	0.299	0.245	0.353
14b	Unet (Vanilla)	**0.719**	0.744	0.701	0.566	**0.251**	0.186	0.317
	Resnet34	0.705	0.737	0.681	0.548	0.265	0.202	0.327
	MobilenetV2	0.693	0.747	0.654	0.535	0.277	0.216	0.339
	Segformer	0.681	0.727	0.648	0.521	0.288	0.230	0.347

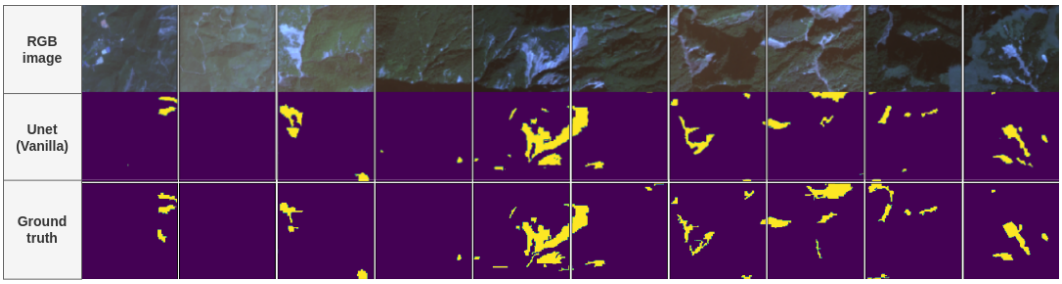

Figure 3: Comparative performance of the top-performing model (Unet-Vanilla) in identifying Landslide and Non-Landslide areas, featuring examples of RGB patches and corresponding ground truth

4 Cloud-based monitoring system framework

4.1 Temporal analysis

The focus of the current study is the resolution of a task within the domain of computer vision. Nonetheless, the efficacy of a monitoring tool is contingent upon temporal variables. For the landslide detection task of this research, we use Sentinel-2 imagery providing new observations every 5 days for a targeted area and limited with the cloud cover which can impede the temporal resolution of image acquisition [15].

Figure 4 elucidates the temporal analysis of imagery from different years over an area of interest, revealing the alterations in surface coverage in locales that have experienced landslides. For each event, ante- and post-event imagery are displayed, thereby integrating a temporal factor into the satellite-based assessment and detection of landslide occurrences. The model used for these predictions were U-net Vanilla with 6 bands and using the full dataset (L4S + L4S-PE) trained previously (Table 3).

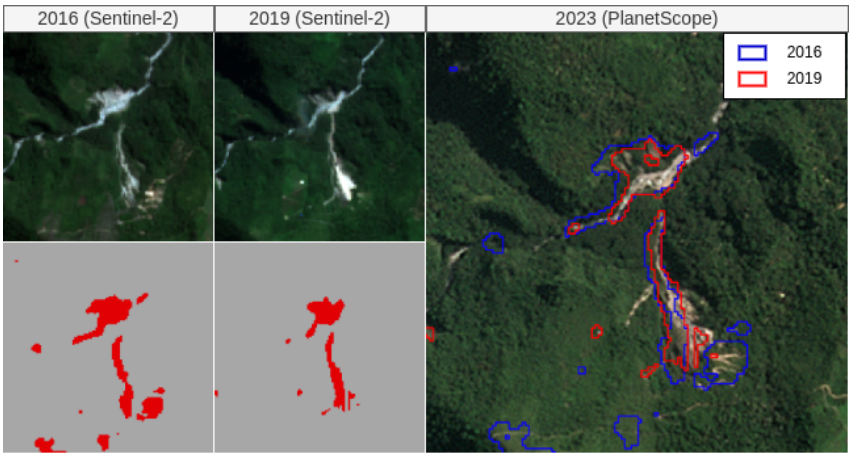

Figure 4: Comparative temporal analysis of various Regions of Interest (ROI) within the Peruvian region

4.2 Monitoring system

The adoption of remote sensing techniques for the monitoring of geographic and environmental phenomena has witnessed an exponential increase internationally [16, 17, 18, 19]. Geographical Information Systems (GIS) have progressively evolved to include cloud-based analyses of satellite imagery. The current investigation leverages the capabilities of Google Earth Engine (GEE), a pioneering cloud-based platform that streamlines cloud service integration, simplifies the download and preprocessing of imagery, and underpins AI-driven segmentation techniques for more sophisticated monitoring endeavors.

4.2.1 Download and imagery processing

Satellite imagery provides a unique view of the terrain and allows early detection of potential landslides. This study works with GEE, which allows filtering and selection tools based on parameters like dates, cloud cover and localization to download Sentinel-2 (L1C) images with a spatial resolution of 10 metres which are available every 5 days for the same location, limited only to the cloud cover of the scene at the time they were captured. On the other hand, Alos Palsar images are not directly in GEE but can be stored in a cloud bucked like Google Cloud Storage (GCS) in Geotiff format.

Working with the Pytorch Lightning framework, it facilitates the dataloader and splitting for an area of interest (aoi) to monitor and links to the pre-trained model to create a map of landslide predictions.

In cases when the area is bigger than the original dimensions, we implemented a stitching process that resembles the prediction in the same size of the aoi evaluated. This process exports the results

in a binary raster with Cloud Optimized Geotiff (COG) format that facilitates the integration with viewers.

Figure 4.2.1 shows the workflow used in this research considering the main parts, data processing, model training and, analysis and application.

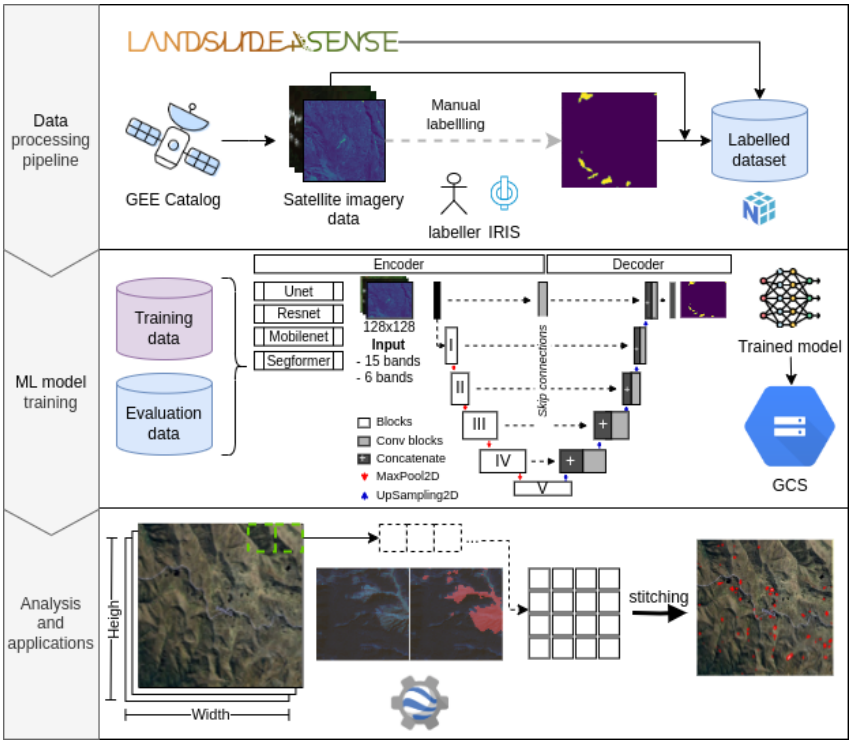

Figure 5: Workflow used of the Landslide Detection System using Sentinel-2 and Alos Palsar Imagery

4.2.2 Cloud-Based integration

To establish a dynamic and scalable landslide monitoring system, the trained semantic segmentation models—designed to differentiate between landslide and non-landslide classes—are securely housed within Google Cloud Storage. This allows for robust and accessible data management. Similarly, other studies have utilized cloud-based architecture and on-the-fly processes with Google services, demonstrating the effectiveness of these approaches in environmental analysis and near real-time monitoring [20]. The backend infrastructure, potentially developed using Google Cloud Functions or analogous cloud services, acts as an intermediary between user interactions or system-driven triggers and the execution of the model's processes. This serverless architecture affords an economical scalability model, engaging resources solely during model inquiries and thus adeptly managing fluctuating workloads without persistent server upkeep.

The automation of the landslide detection workflow leverages satellite data acquisition and processing, utilizing scheduling services to periodically invoke GEE for the latest Sentinel-2 and Alos Palsar imagery pertaining to predefined areas of interest.

Upon the detection of new imagery, the pipeline activates a sequence of prearranged cloud functions to preprocess the data, ensuring compatibility with our deep learning models. The images, once processed, are directed through the semantic segmentation models to ascertain potential landslide areas. This system is not only streamlined for efficiency but also strategically reduces the necessity for manual oversight, thereby expediting the detection process.

It is envisaged that the landslide predictions formulated by the models will be systematically archived in Google Cloud Storage. In doing so, we guarantee that the predictive data remains promptly accessible for in-depth analysis and is readily amenable to integration with web-based visualization interfaces utilizing the Cloud Optimized Geotiff (COG) standard. Consequently, this would furnish

end users, such as disaster response teams, with the capabilities to swiftly visualize and react to landslide incidents.

5 Conclusions

In the continuously evolving field of remote sensing, databases such as Landslide4Sense, which contains pixel-accurately labeled satellite imagery sourced from Sentinel-2 and Alos Palsar, stand as a testament to the power of data-driven solutions. This research elucidates that the fusion of additional data can profoundly amplify the scalability and replicability of machine learning models, rendering them applicable across variegated geographical terrains. This synthesis fosters algorithmic generalization, wherein the resampled data with a 10-meter resolution astutely discerns the nuanced morphological facets of landslides.

Nevertheless, one cannot overlook the intricacies introduced by cloud cover, which often acts as an impediment, complicating data normalization and annotation endeavors. Within the pantheon of deep learning architectures, our chosen U-net model emerges, boasting an F1-score of 75.5% over the 71.65% of the article that used only L4S database. This performance metric, achieved by harnessing all 14 spectral bands and utilizing a synergistic blend of Dice Loss and Weighted Cross-Entropy (WCE) loss functions, sets a benchmark in landslide identification.

For comparative analysis, other encoder structures—namely Resnet34, MobilenetV2, and Segformer—were subjected to evaluation, grounded on pivotal metrics encompassing F1-score and IoU reaching 75.5% and 56.6% respectively. Among these, U-net's superior efficacy in landslide detection underscored the indispensable value of meticulously labeled datasets.

A salient observation was the efficacy of the amalgamated loss function of Weighted Cross-Entropy (WCE) and Dice, proving especially potent for imbalanced data. Notwithstanding the robustness these models exhibit for specific geographical realms, their applicability across diverse geographies remains to be evaluated. Adaptations to geographical conditions and temporal shifts, like seasonal transitions, are influential for the model's accuracy.

While the prowess of deep learning algorithms is undeniable, their true potential remains tethered to the availability of public annotated imagery. This scarcity underscores the imperative to continually augment and refine datasets, which would catalyze the precision and performance of these models in real-world applications.

6 Code Availability

The code required for database generation, associated resource downloads for each ROI, annotation creation, deep learning model training, application construction, and publishing is open-source and available on Github at https://github.com/ryali93/lanslide4sat_pl. Additionally, the evaluated metrics from all conducted experiments are stored and can be accessed via the Weight & Biases tool, hosted on the following web repository: https://wandb.ai/ryali/lanslide4sat_pl.

References

[1] Xuanmei Fan, Gianvito Scaringi, Oliver Korup, A. Joshua West, Cees J. van Westen, Hakan Tanyas, Niels Hovius, Tristram C. Hales, Randall W. Jibson, Kate E. Allstadt, Limin Zhang, Stephen G. Evans, Chong Xu, Gen Li, Xiangjun Pei, Qiang Xu, and Runqiu Huang. Earthquake-induced chains of geologic hazards: Patterns, mechanisms, and impacts. *Reviews of Geophysics*, 57(2):421–503, 2019.

[2] Derly Gómez, Edwin F. García, and Edier Aristizábal. Spatial and temporal landslide distributions using global and open landslide databases. *Natural Hazards*, Mar 2023.

[3] Liping Yang, Joshua Driscol, Sarigai Sarigai, Qiusheng Wu, Haifei Chen, and Christopher D. Lippitt. Google Earth Engine and Artificial Intelligence (AI): A Comprehensive Review. *Remote Sensing*, 14(14):3253, July 2022.

[4] Noel Gorelick, Matt Hancher, Mike Dixon, Simon Ilyushchenko, David Thau, and Rebecca Moore. Google earth engine: Planetary-scale geospatial analysis for everyone. *Remote Sens-*

ing of Environment, 202:18–27, 2017. Big Remotely Sensed Data: tools, applications and experiences.

[5] Vitor C. F. Gomes, Gilberto R. Queiroz, and Karine R. Ferreira. An overview of platforms for big earth observation data management and analysis. *Remote Sensing*, 12(8), 2020.

[6] L.M. Highland and Peter Bobrowsky. *The landslide handbook—A guide to understanding landslides*. 2008.

[7] Boletín estadístico virtual de la gestión reactiva del indeci - 2023. Virtual, 2 2023.

[8] Omid Ghorbanzadeh, Yonghao Xu, Pedram Ghamisi, Michael Kopp, and David Kreil. Landslide4Sense: Reference Benchmark Data and Deep Learning Models for Landslide Detection, June 2022. arXiv:2206.00515 [cs, eess].

[9] JAXA/METI ASF DAAC. Alos palsar radiometric terrain corrected low resolution, 2015.

[10] Cesar Aybar, Luis Ysuhuaylas, Jhomira Loja, Karen Gonzales, Fernando Herrera, Lesly Bautista, Roy Yali, Angie Flores, Lissette Diaz, Nicole Cuenca, Wendy Espinoza, Fernando Prudencio, Valeria Llactayo, David Montero, Martin Sudmanns, Dirk Tiede, Gonzalo Mateo-García, and Luis Gómez-Chova. Cloudsen12, a global dataset for semantic understanding of cloud and cloud shadow in sentinel-2. *Scientific Data*, 9(1):782, Dec 2022.

[11] Francis Alistair and John Mrziglod. Intelligence for image segmentation (iris). `https://github.com/ESA-PhiLab/iris`, 2019. Version 1.0.0.

[12] S. R. Meena, L. Nava, K. Bhuyan, S. Puliero, L. P. Soares, H. C. Dias, M. Floris, and F. Catani. Hr-gldd: A globally distributed dataset using generalized dl for rapid landslide mapping on hr satellite imagery. *Earth System Science Data Discussions*, 2022:1–21, 2022.

[13] Olaf Ronneberger, Philipp Fischer, and Thomas Brox. U-net: Convolutional networks for biomedical image segmentation, 2015.

[14] William Falcon et al. Pytorch lightning. `https://github.com/PyTorchLightning/pytorch-lightning`, 2020.

[15] Tomáš Řezník, Jan Chytrý, and Kateřina Trojanová. Machine learning-based processing proof-of-concept pipeline for semi-automatic sentinel-2 imagery download, cloudiness filtering, classifications, and updates of open land use/land cover datasets. *ISPRS International Journal of Geo-Information*, 10(2), 2021.

[16] Yang Hong, Robert F. Adler, Andrew Negri, and George J. Huffman. Flood and landslide applications of near real-time satellite rainfall products. *Natural Hazards*, 43(2):285–294, October 2007.

[17] Leijin Long, Feng He, and Hongjiang Liu. The use of remote sensing satellite using deep learning in emergency monitoring of high-level landslides disaster in jinsha river. *The Journal of Supercomputing*, 77(8):8728–8744, Aug 2021.

[18] Wenjie Li, Jingfeng Huang, Lingbo Yang, Yan Chen, Yahua Fang, Hongwei Jin, Han Sun, and Ran Huang. A practical remote sensing monitoring framework for late frost damage in wine grapes using multi-source satellite data. *Remote Sensing*, 13(16), 2021.

[19] Ali Jamali and Masoud Mahdianpari. A cloud-based framework for large-scale monitoring of ocean plastics using multi-spectral satellite imagery and generative adversarial network. *Water*, 13(18), 2021.

[20] John Burns Kilbride, Ate Poortinga, Biplov Bhandari, Nyein Soe Thwal, Nguyen Hanh Quyen, Jeff Silverman, Karis Tenneson, David Bell, Matthew Gregory, Robert Kennedy, and David Saah. A near real-time mapping of tropical forest disturbance using sar and semantic segmentation in google earth engine. *Remote Sensing*, 15(21), 2023.